Tonkie Khimicheskie Tekhnologii = Fine Chemical Technologies.
2026;21(1):18–29 ISSN 2686-7575 (Online)

Chemistry and technology of organic substances
Химия и технология органических веществ

UDC 541.64+546.284-31+547.424
https://doi.org/10.32362/2410-6593-2026-21-1-18-29
EDN VEYWWH

RESEARCH ARTICLE

Hydrolysis of tetraethoxysilane in various associated media of diols

Alevtina M. Bondareva✉, **Igor I. Pashkin, Alexander V. Krylov**

MIREA – Russian Technological University (M.V. Lomonosov Institute of Fine Chemical Technologies), Moscow, 119454 Russia

✉ *Corresponding author, e-mail: bondaalevtina@yandex.ru*

Abstract

Objectives. To investigate the specific features of tetraethoxysilane (TEOS) hydrolysis in associated media of saturated diols and their esters in acidic media. Propylene- and butylene glycols and ethylcarbitol were selected as associated systems.

Methods. Association, hydrolysis, and condensation processes in the TEOS–diol system were studied by potentiometry, infrared spectroscopy, and dynamic light scattering in liquid media. The acidic environment was created by adding HCl in the amount not exceeding 0.3 wt %.

Results. The hydrolysis of TEOS in associated alcohol media is limited by the reaction that yields silanol $(RO)_3SiOH$, which further interacts with the associated diol. This results in the incorporation of $(RO)_3SiO$ groups into the hydrogen bond network of diols. This is confirmed by a decrease in the self-association of diols with a decrease in size in the diol–$(RO)_3SiO$ domains of up to 1–7 μm.

Conclusions. The use of diols as a reaction medium for TEOS with a low content of H_2O in acidic media limits the depth of hydrolysis and condensation, which increases the possibility of esterification reactions of diol with alkoxy derivatives of silanols. The decreased number of hydroxyl groups during the transition from diols to their esters has a significant effect on the degree of association.

Keywords

association, diffusion coefficient, diols, IR spectroscopy, hydrodynamic radius, hydrolysis, laser diffraction, tetraethoxysilane

Submitted: 05.07.2024
Revised: 18.09.2025
Accepted: 15.01.2026

For citation

Bondareva A.M., Pashkin I.I., Krylov A.V. Hydrolysis of tetraethoxysilane in various associated media of diols. *Tonk. Khim. Tekhnol. = Fine Chem. Technol*. 2026;21(1):18–29. https://doi.org/10.32362/2410-6593-2026-21-1-18-29

НАУЧНАЯ СТАТЬЯ

Гидролиз тетраэтоксисилана в ассоциированных средах предельных диолов и их эфиров

А.М. Бондарева✉, И.И. Пашкин, А.В. Крылов

МИРЭА – Российский технологический университет (Институт тонких химических технологий им. М.В. Ломоносова), Москва, 119454 Россия

✉ *Автор для переписки, e-mail: bondaalevtina@yandex.ru*

Аннотация

Цели. Исследование особенностей процесса гидролиза тетраэтоксисилана (ТЭОС) в ассоциированных средах предельных диолов и их эфиров в кислых условиях. В качестве ассоциированных систем были выбраны пропилен- и бутиленгликоль, а также этилкарбитол.

Методы. Исследование процессов ассоциации, гидролиза и конденсации в системе ТЭОС–диолы проводили методами потенциометрии, инфракрасной спектроскопии и динамического рассеяния света в жидких средах. Кислотность среды обеспечивалась добавлением не более 0.3 мас. % HCl.

Результаты. Гидролиз ТЭОС в ассоциированных спиртовых средах лимитируется протеканием реакции образования силанола $(RO)_3SiOH$, который в дальнейшем взаимодействует с ассоциированным диолом, что приводит к встраиванию групп $(RO)_3SiO$ в сетку водородных связей диолов. Это подтверждается снижением самоассоциации диолов с уменьшением размера в доменах диол–$(RO)_3SiO$ до 1–7 мкм.

Выводы. Использование в качестве реакционной среды диолов для ТЭОС при малом содержании H_2O в кислых средах ограничивает глубину гидролиза и конденсации, что увеличивает возможность протекания реакций этерификации диола алкоксипроизводными силанолов. Большой эффект на степень ассоциации оказывает уменьшение числа гидроксильных групп при переходе от диолов к их эфирам.

Ключевые слова

ассоциация, гидродинамический радиус, гидролиз, диолы, ИК-спектроскопия, коэффициент диффузии, лазерная дифракция, тетраэтоксисилан

Поступила: 05.07.2024
Доработана: 18.09.2025
Принята в печать: 15.01.2026

Для цитирования

Бондарева А.М., Пашкин И.И., Крылов А.В. Гидролиз тетраэтоксисилана в ассоциированных средах предельных диолов и их эфиров. *Тонкие химические технологии*. 2026;21(1):18–29. https://doi.org/10.32362/2410-6593-2026-21-1-18-29

INTRODUCTION

Currently, sol–gel technology is widely used for producing transparent, shape-stable hybrid materials (HMs). The as-obtained materials enable the incorporation of organic groups into inorganic systems [1]. When optimizing synthesis conditions, HMs with unique, synergetic characteristics can be obtained, with their properties outperforming those of each individual component [2, 3].

The sol–gel process also enables the production of improved materials with high purity and homogeneity under relatively mild conditions. The exceptional properties of such materials are explained by the extended polymer-nanofiller interfacial area and are determined by the strength of interfacial interactions. Furthermore, polymer hybrids exhibit optical transparency due to the small area of heterogeneity domains [4, 5].

The main advantage of sol–gel technology, which encompasses hydrolysis and condensation processes, lies in its capacity to tailor the synthesis by varying and monitoring the reaction parameters (e.g., pH, catalyst nature, temperature, and/or reagent ratios) [3]. The formation of gels with controlled nanoscale architecture, unique morphology, and properties under mild reaction conditions [6] accounts for their wide range of applications, e.g., as hybrid coatings [7], biohybrids [8], and materials for medicinal purposes [9].

Gels based on silicic acid occupy a significant place among gel materials. These are porous, elastic materials with a 3D polymer network, the pores of which are primarily filled with solvent molecules or, in the case of hydrogels, with water, typically up to 70–99% [10].

The number of biomedical applications for hydrogels is rapidly increasing due to their outstanding physical, structural, and mechanical properties. The silicic acid polymer network, filled with water, imparts unique characteristics to hydrogels, rendering them particularly attractive for applications in biomedical engineering [10–13].

The formation of a 3D siloxane network during the synthesis of hybrid sol–gel materials and the subsequent polymerization of the resulting dispersed silicic acid particles lead to the capillary-porous structure of the elastic gel [14].

The strategy for synthesizing hybrid sol–gel materials is represented mainly by two synthetic pathways [3, 14–15]:

- one-stage synthesis in an alkaline medium (co-condensation);
- two-stage synthesis, where the first hydrolysis stage primarily occurs under acidic conditions, while the second stage of alkaline condensation is conducted separately (silylation).

The key difference between these two strategies consists in the degree of incorporation of organic groups, which attach to the internal and external pore walls during their formation.

In the two-stage synthesis, after pore formation, the organic modifier in the silylation stage attaches only to the external pore walls. This increases the limit of organic solvent incorporation to 40% or greater [9]. In these systems, interfacial properties play an essential role in determining the functional properties of the material. Depending on the type of interface, the sol–gel process enables the formation of two main classes of HMs.

In the first class of materials, inorganic and organic components are connected by weak (non-covalent) bonds, including ionic interactions, hydrogen bonds (H-bonds), van der Waals forces, and π–π interactions [1]. The cases in point include rhodamine 6G [16] or enzymes [17] formed through encapsulation of an organic molecule within the formed cavities of an inorganic matrix. In the second class of materials, the embedded phase is firmly bound by chemical bonds to the silicon matrix of the gel.

The sol–gel process can be managed by a known method involving the use of organic components as templates [18–21] to obtain final products whose properties are determined by the organic–inorganic interface. Depending on the intended use of the product, the template or sacrificial spacer can be chemically removed, leaving voids with a specific pore size [20].

Various methods for optimizing synthesis using a wide range of solvents, surfactants, and natural products have been discussed in the literature [22, 23]. In this regard, highly associated alcohols [24] and polyols [25], which possess a strong internal network of hydrogen bonds, can be of interest as solvents. Alkoxysilanes, including tetraethoxysilane (TEOS), are predominantly used for obtaining inorganic structures. TEOS is one of the most common precursors for forming a silica network *in situ* within an organic matrix.

The synthesis of silicic acid gels comprises a stage involving the hydrolysis of silicon alkoxides dissolved in various alcohols, ROH, in the presence of mineral acid or base catalyst (Eq. 1), and subsequent condensation reactions involving silanol groups, resulting in the formation of siloxane bonds and byproducts, which are water molecules (Eq. 2) or alcohol (Eq. 3):

$$Si(OR)_4 + H_2O \rightarrow (RO)_3SiOH + ROH, \quad (1)$$

$$(RO)_3SiOH + HOSi(OR)_3 \rightarrow (RO)_3SiOSi(OR)_3 + H_2O, \quad (2)$$

$$Si(OR)_4 + HOSi(OR)_3 \rightarrow (RO)_3SiOSi(OR)_3 + ROH, \quad (3)$$

$$Si(OR)_4 + nR'OH \rightarrow (R'O)_zSi(OR)_{4-n} + nROH, \quad (4)$$

$$(RO)_3SiOH + nR'OH \rightarrow (R'O)_zSi(OR)_{4-n} + nH_2O. \quad (5)$$

The sol–gel process is sensitive to the nature of the catalyst. Acidic catalysts primarily promote the hydrolysis process, while basic catalysts are capable of facilitating the polycondensation process [3]. The choice of a catalyst determines the growth mechanism of silica domains, thus being an important factor for filler dispersion. In most cases, the morphology of the final product is controlled by the type of the catalyst used. Acid-catalyzed reactions lead to the formation of a 3D gel or network structure [26, 27], while base-catalyzed reactions result in the formation of condensed spherical particles [28, 29].

Previous research showed the hydrolysis stage (Eq. 1) to be the limiting step for particle formation not only in alkaline media [30–32] but also in acid-catalyzed systems [33, 34].

In comparison with other components in sol–gel systems, the alcohol solvent plays a rather complex role. The nature and content of the alcohol are significant from the standpoint of the solubility of intermediates containing polar and charged groups [34]. Alongside regulating the system miscibility, the alcohol used in the synthesis process can act as a reagent in transesterification reactions (Eq. 4). According to the study [34], for low-molecular-weight alcohols, such as methanol and ethanol, transesterification of TEOS is negligible and largely determined by the water/alcohol ratio.

During the synthesis of silicic acid gels in an alcohol solvent medium, stages of silylation of ROH by alkoxysilanols (Eq. 5) can also occur.

Previously, the use of ^{29}Si and ^{13}C nuclear magnetic resonance and small-angle X-ray scattering methods [35, 36] established that the rates of condensation stages decrease in an alkaline medium when transitioning from the initial TEOS monomer to a dimer with a siloxane bond. When the reaction proceeds in methanol or ethanol, transesterification between methanol and TEOS was found to occur (Eq. 4),

although being negligible compared to the formation of hydrolyzed intermediates (Eq. 1). The authors believe that the differences in the sizes of silicon-containing particles in the reactions conducted in methanol or ethanol are due to thermodynamic interactions between the solvent and the hydrolyzed intermediates of a silanol nature.

In the study [37], the influence of the solvent on the kinetics of the initial hydrolysis stage was investigated from the perspective of solvent polarity and hydrogen bond formation. It was shown that the initial hydrolysis rate and the average particle size increase with an increase in the molecular weight of primary alcohols. For secondary alcohols, the hydrolysis rate decreases while particle size increases.

The study [38] investigated the influence of various alcohols on the reaction rates and particle sizes of silica synthesized via TEOS hydrolysis and condensation. Silica particles ranging in size from 100 nm to 2 μm were obtained by varying the ROH composition, where R = C_nH_{2n+1} with *n* values from 1 to 15. The reactions proceed fastest in an ethanol/decanol mixture at a ratio of about 1 : 1 and slowest in pure ethanol. The authors established that both the hydrolysis rate and the condensation rate increase with a decrease in solvent polarity. At the same time, no correlation between polarity and rate constants was observed.

A number of studies have shown that alkoxy exchange is activated in an acidic medium, while it cannot be detected in basic media [33, 39]. However, in a work by Lima *et al.* [40], the possibility of rapid exchange of alkoxy groups at an early stage of TEOS hydrolysis in a basic medium was established. Under these conditions, both the reaction rate and the size of the resulting silica particles undergo a significant change.

Knowledge of the phase interface structure in organic–inorganic hybrid materials obtained via sol–gel processes makes it possible to tailor the structure and properties of silicic acid gels, which is extremely important for the synthesis of new, promising materials.

Associated media are characterized by strong intermolecular binding through hydrogen bonds or dipole and ion–dipole interactions, e.g., in polyvinylpyrrolidone. Systems with strong hydrogen bonds include saturated 1,2- and 1,3-diols, triols, polyols, and their ethers.

This paper presents the results of TEOS hydrolysis in diols: 1,3-propylene glycol (PG), 1,3-butylene glycol (BG), and the monoethyl ether of diethylene glycol, i.e., ethyl carbitol (EC), using infrared (IR) spectroscopy and dynamic light scattering (DLS) methods in an acidic medium. The acidic medium was ensured by the addition of HCl. The H_2O concentration was determined solely by the water content in the initial diols and/or the water introduced with HCl, non exceeding 0.3 wt %.

EXPERIMENTAL

In this work, the following chemical compounds were used:

- 1,3-Butylene glycol (*KhimFarm*, Russia) (CAS No. 107-88-0), main substance content not less than 99.5%;
- 1,3-Propylene glycol (*NOVATORKHIM*, Russia) (CAS No. 504-63-2), 99.95%;
- Ethyl carbitol (2-(2-ethoxyethoxy)ethanol) (*BIOAMIN-RUS*, Russia) (CAS No. 111-90-0), Technical Specification TU 2422-125-05766801-2003, premium grade, main substance content not less than 99%, ethylene glycol content is 0.8%;
- Tetraethoxysilane (tetraethyl silicate) (*EKOS-1*, Russia) (CAS No. 78-10-4), Technical Specification TU 2435-419-05763441-2003, main substance content not less than 99.5%, ethyl alcohol content is no more than 0.10%;
- HCl (*KHIMMED*, Russia);
- Distilled water H_2O (Russia, RTU MIREA, M.V. Lomonosov Institute of Fine Chemical Technology, Ya.K. Syrkin Department of Physical Chemistry), GOST R 58144-2018[1].

IR spectra of samples in liquid and solid forms were recorded on a Cary 630 FTIR spectrometer (*Agilent Technologies*, USA) using a single-bounce diamond attenuated total reflectance accessory in the range of 4000–350 cm^{-1} with a spectral resolution of <2 cm^{-1}. Processing of the IR spectra was performed using the Agilent MicroLab software (*Agilent Technologies*, USA).

DLS spectra were recorded using a Photocor Compact-Z instrument (*Photocor*, Russia). The power of the thermostabilized semiconductor laser (638 nm) was 25 mW. Particle size measurements were conducted at angles of 90° and 160° at a constant temperature of 25°C. Measurements in concentrated and opaque systems were performed using the backscattering method at an angle of 160°. Signal analysis was carried out by the built-in Photocor FC correlator for auto- and cross-correlation measurements. Processing of DLS spectra was performed using the DynaLS software package by Photocor.

[1] GOST R 58144-2018. National Standard of the Russian Federation. Distilled water. Specifications. Moscow: Standartinform; 2018. URL: https://cdn.termexlab.ru/files/4385340a/f801/428e/9766/de94c9e1741c.pdf. Accessed July 01, 2019 (in Russ.).

Potentiometric pH determination was carried out using an Expert-001 ionometer (*Ekoniks-Expert*, Russia) with a measurement range of pH 0–14, using a combined glass electrode IT ESK 10601 7. The limit of permissible basic absolute measurement error was ΔpH 0.03.

Preparation of reaction mixtures

Reaction mixtures with a volume of 50 mL were prepared by direct mixing of glycols or EC (94–95 wt %) with a constant amount of TEOS (5 wt %) under vigorous stirring at room temperature (25°C). An HCl solution was added as an acid catalyst. The pH value of the reaction mixture was maintained constant (pH 2.1–2.5). The total water content in the reaction mixture was determined by the amount of water in the initial glycols and the amount of water introduced with the HCl solution, not exceeding 1–2 wt %.

The solutions were transparent and similar in viscosity to the diols.

For reaction mixtures based on EC in the EC–TEOS system, solution opalescence with a whitish tint was observed.

The obtained reaction mixtures were analyzed using IR spectroscopy and DLS methods over a time interval of up to 48 days.

RESULTS AND DISCUSSION

In the IR spectrum of PG diol (Fig. 1), alcohol association is manifested by the broadening of the bands of O–H bond stretching vibrations ν(OH) = 3320 cm^{-1}, as well as C–H bonds in CH_2, CH_2–O groups in the region ν = 2867–2969 cm^{-1} and deformation vibrations of these groups in the region δ = 1457–1260 cm^{-1}. This agrees with data on the formation of a hydrogen bond network in diols [41]. C–O bond stretching vibrations appear in the region of 1125–1000 cm^{-1} in the form of two sets: a broadened band at 1036 cm^{-1} for the associated form of diols and two narrow bands at 1135 and 1075 cm^{-1}. Similar results are observed for BG, although with a slight difference.

Diols always contain a residual amount of water, with a band of O–H bond stretching vibrations ν(OH) = 3430 cm^{-1} overlapping with the ν(OH) band of the diols and water deformation vibrations at 1645 cm^{-1}.

In the IR spectrum of EC, due to the increased content of CH_2–O groups compared to PG, the intensity and width of the hydroxyl OH^- group vibration band at 3320 cm^{-1} is significantly reduced, and the intensity of the C–H bond stretching vibration bands at ν = 2867 cm^{-1} increases. This confirms a decrease in the degree of association of EC compared to diols. It should also be noted that instead of two narrow bands at 1135 and 1075 cm^{-1}, a single combined band at 1105 cm^{-1} is observed.

The presence of different forms of diol associates and silicon-containing products is confirmed by the obtained DLS spectra.

In the DLS spectrum of PG (Fig. 2a), two signals are observed: a fast mode (F1) and a slow mode (S1), with an average hydrodynamic radius for S1 of r_g = 11 μm and a ratio of F1 : S1 = 1 : 3. Thus, it can be assumed that the two forms of CO stretching vibrations correspond to the fast (F1, ν = 1135 cm^{-1}) and slow (S1, ν = 1075 cm^{-1}) modes of motion.

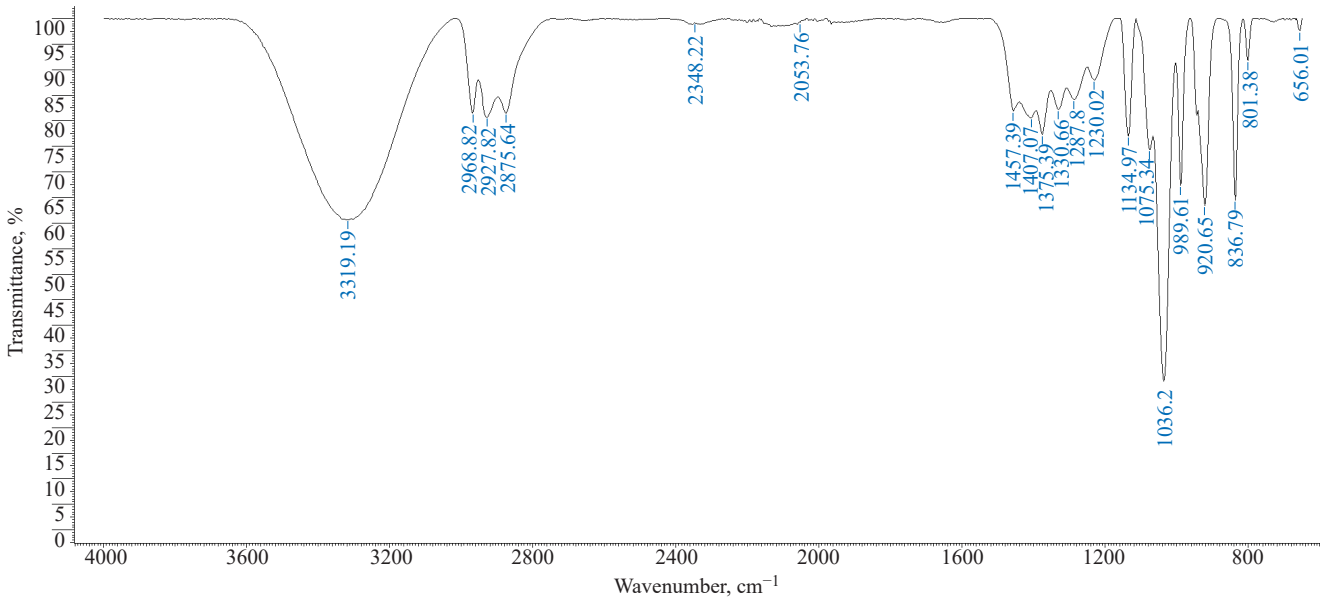

Fig. 1. Infrared spectrum of PG

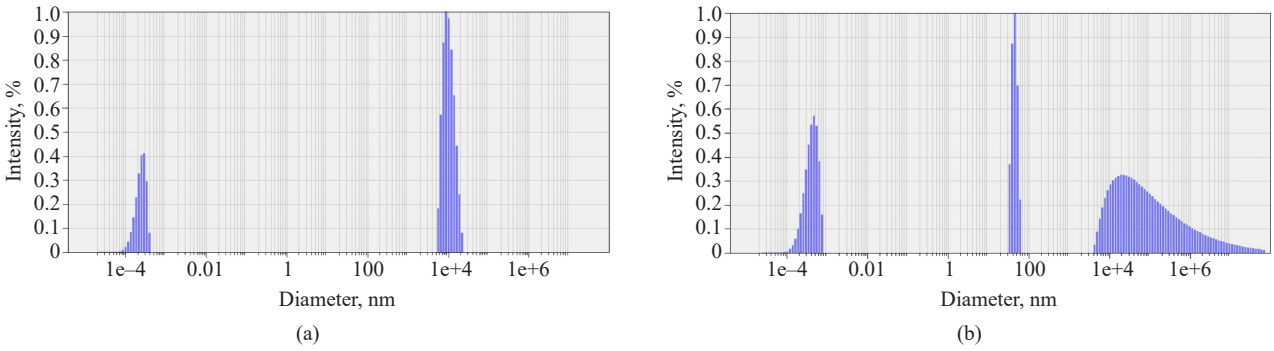

Fig. 2. DLS spectra of (a) PG, (b) EC

The substitution of PG with EC affects the appearance of the entire spectrum. The decrease in the degree of association for EC (Fig. 2b) leads to an increase in the contribution of the fast mode F1 and a decrease in the contribution of the slow modes S. At the same time, the slow mode splits into two components: S1 (ν = 1105 cm^{-1}) and S2 (ν = 1062 cm^{-1}) with diffusion coefficients of $D_{S1} = 5.3 \cdot 10^{-8}$ cm^2/s and $D_{S2} = 8.1 \cdot 10^{-11}$ cm^2/s.

In this work, the process of TEOS hydrolysis and condensation was monitored by changes in viscosity, IR spectra, and phase composition, as assessed by DLS spectra of the reaction system.

PG + TEOS system

The structures of TEOS and diols are largely similar due to the presence of the C–O bond. This is confirmed by the appearance of bands corresponding to C–H bond stretching vibrations in the CH_2 and CH_3 alkoxy groups and deformation vibrations of the $–CH_2–O$ groups in the regions similar to those for diols (Fig. 1). The absence of associations between TEOS molecules results in noticeably narrower vibration bands compared to PG. A distinctive feature of the alkoxy groups in TEOS is the presence of Si–O bond stretching and deformation vibration bands at 1072, 958, and 785 cm^{-1} of comparable intensity. Furthermore, similar to diols, the presence of two sets of silicon alkoxide derivatives is observed: a broadened band at 1072 cm^{-1} and two narrow bands at 1167 and 1100 cm^{-1}. It can be seen from Fig. 3 that the IR spectrum at the onset of the experiment represents the sum of the glycol and TEOS spectra. Thus, the difference in the alkoxy groups of diols and TEOS is observed in the shift of the wavenumbers of the vibration bands: 1135 → 1167 cm^{-1}, 1075 → 1100 cm^{-1}, and 1038 → 1072 cm^{-1}.

In the DLS spectrum of TEOS (Fig. 4), a small number of oxysilicon particles with r_g = 93 nm, dissolved in TEOS, is observed, along with a broadened signal of the slow mode S. This can be explained by an impurity of a partially hydrolyzed product (due to atmospheric moisture) with $D_S = 5.8 \cdot 10^{-10}$ cm^2/s.

The addition of 3 to 5 wt % TEOS to diols at pH 2.5 leads to a noticeable change in the IR and DLS spectra. First of all, practically immediately after mixing, a narrowing of the C–H bond stretching vibration bands in the CH_3, $CH_2–O$ groups in the region ν = 2867–2969 cm^{-1} and the bands of deformation vibrations of these groups in the region δ = 1457–1260 cm^{-1} is observed in the IR spectrum for PG (Fig. 3). This indicates a decrease in the degree of association of the initial diol.

Following aging for 48 days, the reaction mixture remains close to homogeneous, and the IR spectrum shows a noticeable decrease in the intensity of the TEOS vibration bands at 958 and 785 cm^{-1}, indicating hydrolysis of the alkoxysilane.

For BG, replacing the H atom with a methyl radical in the CH_2OH group of PG increases the hydrophobicity of the diol and reduces its self-association. This is manifested in the narrowing of the bandwidth of the O–H stretching vibration at ν(OH) = 3320 cm^{-1}. At the same time, broadening of the C–H bond stretching vibration band in the CH_3, $CH_2–O$ groups in the region ν = 2867–2969 cm^{-1} is maintained. The persistence of the stretching vibration bands for TEOS confirms a decreased hydrolysis rate compared to PG.

EC + TEOS

A different picture is observed for the less associated EC. The addition of TEOS to EC at pH 2.5 produces a negligible effect on the appearance of the IR spectrum (Fig. 5). It is only after aging the EC + TEOS reaction mixture for 48 days that a narrowing of the C–H bond stretching vibration bands in the CH_3, $CH_2–O$ groups in the region ν = 2867–2969 cm^{-1}, and the bands of deformation vibrations of these groups in the region δ = 1457–1260 cm^{-1} are observed. At the same time, the intensity of the bands characteristic of TEOS remains

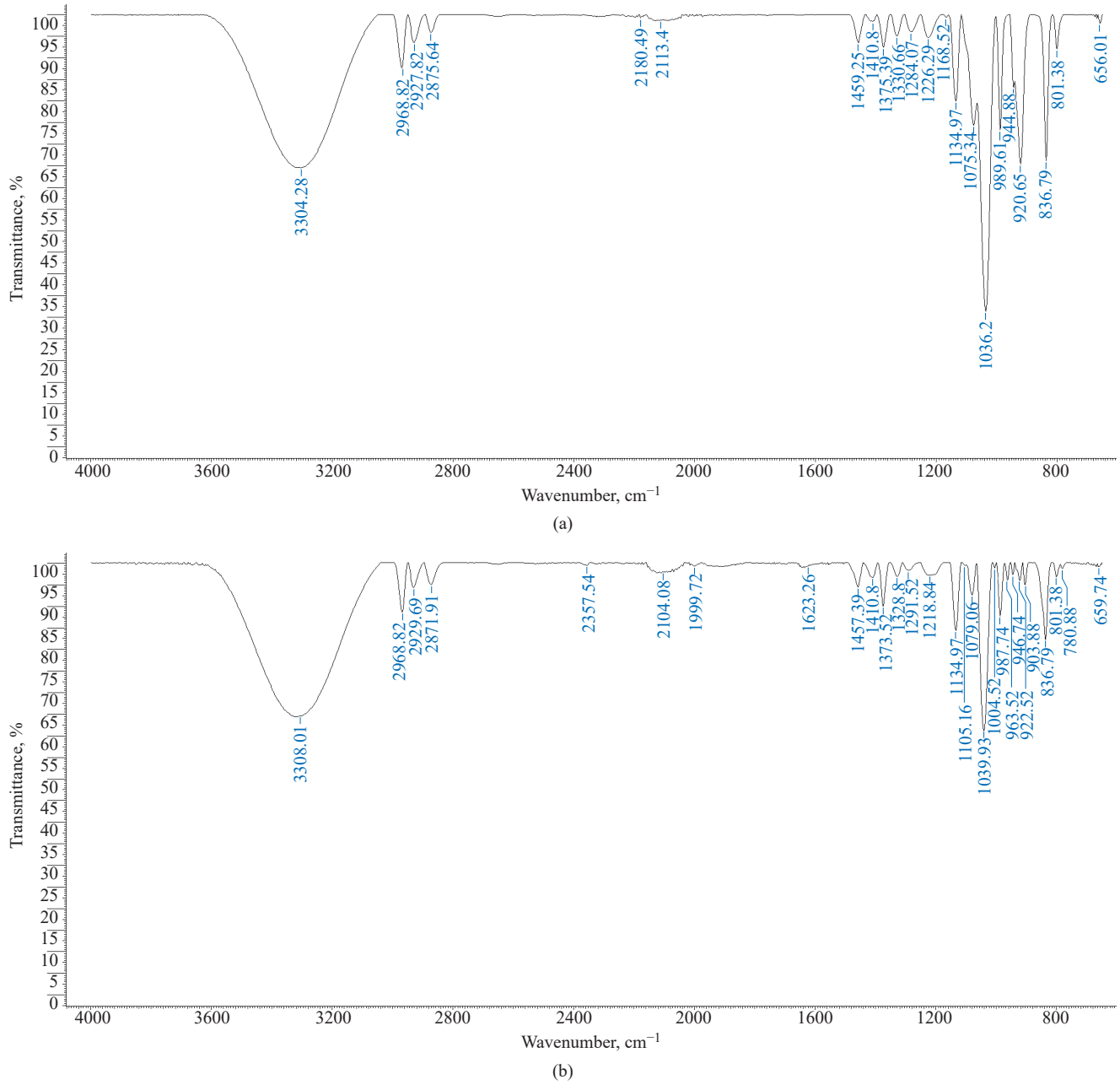

Fig. 3. IR spectra of PG + TEOS mixture: (a) immediately after mixing, (b) after 48 days

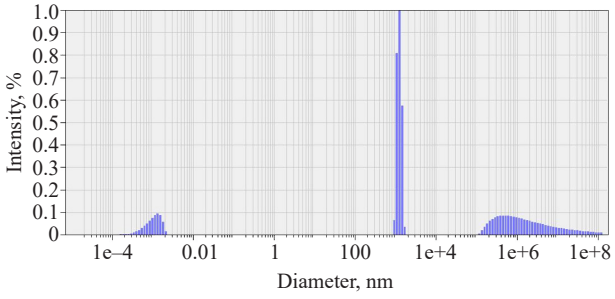

Fig. 4. DLS spectrum of TEOS

almost unchanged, indicating a decreased rate of hydrolysis and condensation for the EC ether compared to the saturated diols.

For all studied diols, the reaction mixture generally remains homogeneous. However, the onset of its phase separation is observed. The H–O–H deformation vibration band at 1645 cm^{-1} splits into two bands at 1623 and 1649 cm^{-1}. According to the authors [34], bands corresponding to Si–OH group vibrations may also appear in this region, which is consistent with the slower TEOS hydrolysis process in EC.

The studies [1, 6] reported that the formation of the primary silanol $(RO)_3SiOH$ remains the limiting stage of hydrolysis even under an excess of water in an acidic medium. Given the extremely low water content in the system, the obtained results can be explained not only by the condensation reaction with the formation of a siloxane bond (Eqs. 2 and 3) but also by a significant contribution from the esterification reaction of the resulting silanol derivatives of diols. This leads to the incorporation of alkoxysilanolic groups into the hydrogen bond network of the diols:

$$2(RO)_3SiOH + HO(CH_2)_nOH \rightarrow \rightarrow (RO)_3SiO–O(CH_2)_nO–Si(OR)_3 + 2H_2O \quad (6)$$

The possibility of transesterification of the initial TEOS in a 95–97% diol medium cannot be ruled out. This should also lead to the incorporation of alkoxysilanols into the hydrogen bond network of the diols:

$$2Si(RO)_4 + HO(CH_2)_n(OH) \rightarrow \rightarrow (RO)_3SiO(CH_2)_nOSi(RO)_3 + 2ROH \quad (7)$$

Thus, the reactions according to Eqs. (6) and (7) proceed for diols, being unlikely for monohydric alcohols. The result of silylation of diols should lead to a decrease in their association (Fig. 6), forming smaller domains, which we observe in the DLS spectra.

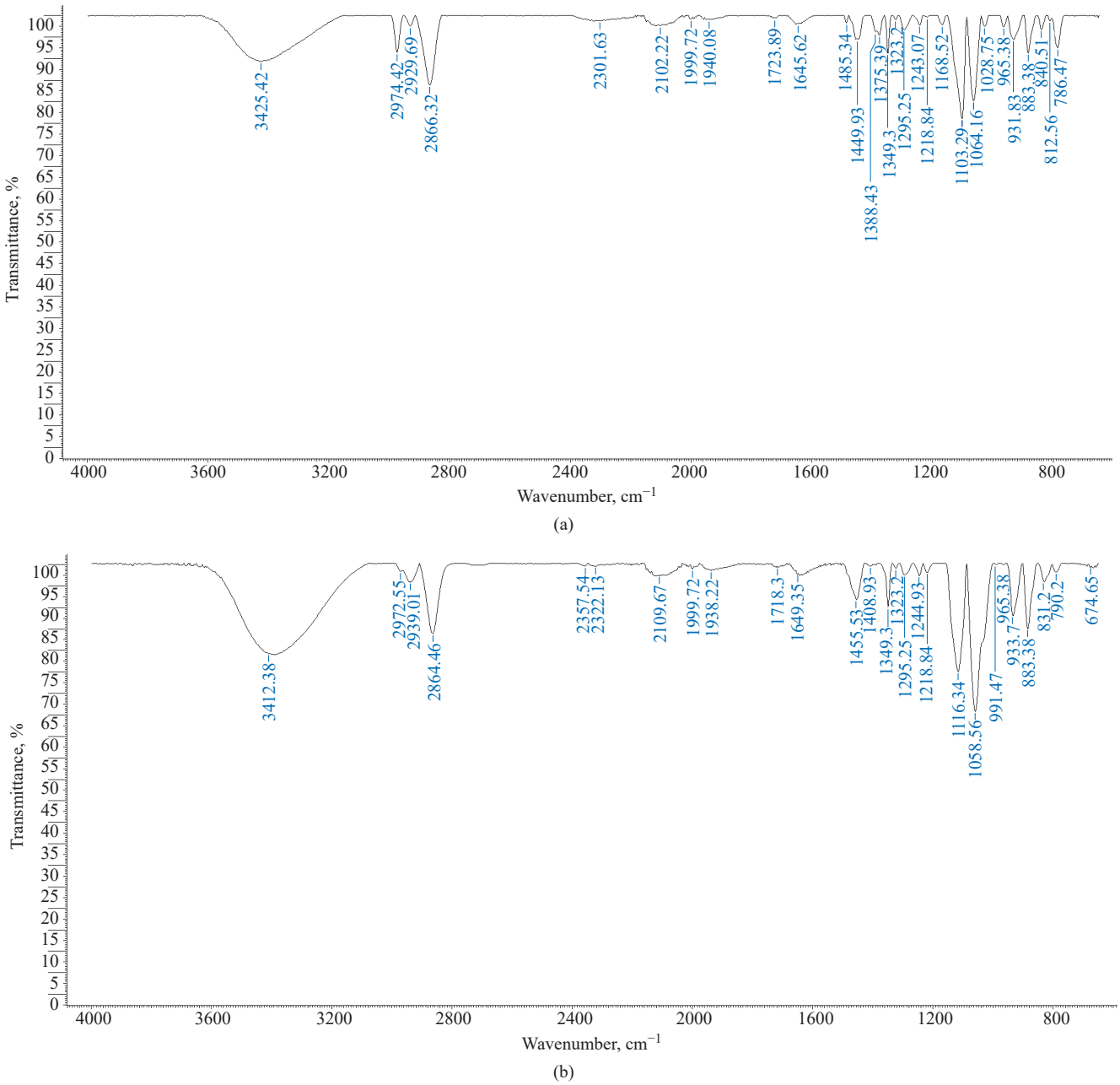

Fig. 5. IR spectra of EC + TEOS mixture: (a) immediately after mixing, (b) after 48 days

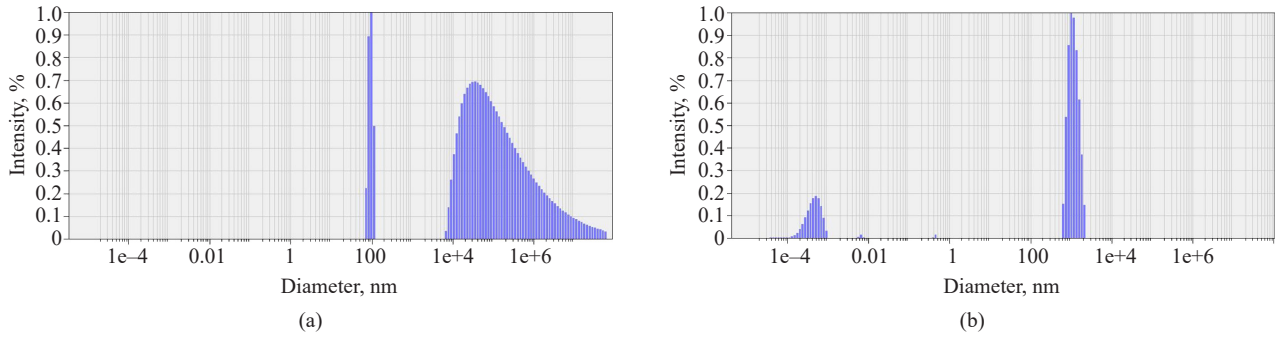

Fig. 6. DLS spectra of a mixture of PG + 5% TEOS: (a) immediately after mixing, (b) 48 days after mixing

Immediately after mixing saturated diol PG with 5 wt % TEOS (Fig. 6a), the fast mode F1 was not observed, while the slow mode signal split into two, S1 and S2, with diffusion coefficients $D_{S1} = 2.2 \cdot 10^{-8}$ cm²/s and $D_{S2} = 4.4 \cdot 10^{-11}$ cm²/s.

After the period of 48 days, the DLS spectrum of the system (Fig. 6b) showed signals for the fast mode F1 (19%) and a narrow monomodal signal of the slow mode S (r_g = 1.17 μm; $D_S = 2.3 \cdot 10^{-9}$ cm²/s). The significant reduction in the size of the associates and the diffusion coefficients fully confirms the aforementioned statement.

A similar result with a narrow monomodal signal of the slow mode S is observed for BG after 48 days, confirming the incorporation of alkoxysilanols into the hydrogen bond network. At the same time, larger domains with a smaller diffusion coefficient for the slow mode S (r_g = 7.18 μm; $D_S = 3.7 \cdot 10^{-10}$ cm²/s) are observed compared to S for PG (r_g = 1.17 μm; $D_s = 2.3 \cdot 10^{-9}$ cm²/s). However, this does not contradict the previous conclusion.

In comparison with PG diol, the decrease in the number of hydroxyl groups when moving to EC has a negligible effect on the appearance of the IR spectrum (Fig. 5).

The rate of hydrolysis/condensation in the EC–TEOS system substantially differs from the rate of reactions involving diols. After aging the EC–TEOS mixture for 48 days (Fig. 7), an increase in the viscosity of the reaction mixture is observed, producing bands characteristic of siloxane bonds in the IR spectra (Fig. 5). The intensity of the fast mode F1 signal is 19.9%. The diffusion coefficients of the two slow modes have practically remained unchanged: 9.3% S1, $D_{S1} = 3.0 \cdot 10^{-9}$ cm²/s and 70.3% S2, $D_{S2} = 4.5 \cdot 10^{-11}$ cm²/s. However, the size of the associate involving alkoxysilicon components of the slow mode S1 increased almost tenfold (to r_g = 840 nm) compared to PG (r_g = 93 nm) at the initial moment of contact. Thus, the decrease in diol association leads to two processes: less active incorporation into the hydrogen bond network and the growth of agglomerates of siloxane condensation products of TEOS.

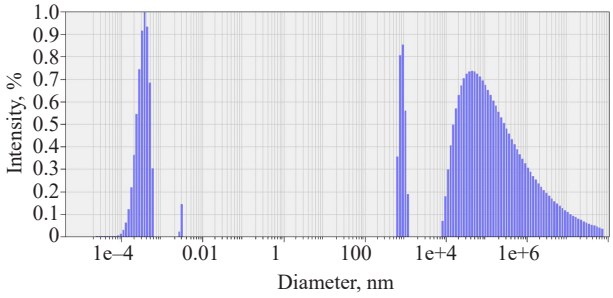

Fig. 7. DLS spectrum 48 days after mixing EC + 5% TEOS

CONCLUSIONS

The use of diols as a reaction medium for TEOS hydrolysis, under conditions of low H_2O content in acidic media, limits the extent of hydrolysis and condensation, while increasing the possibility of esterification reactions between the diols and alkoxy derivatives of silanols. The incorporation of $(RO)_3SiO$ groups into the hydrogen bond network of the diols reduces diol association and decreases domain sizes to 1–7 μm. The decrease in the number of hydroxyl groups in diol ethers has a significant effect on the degree of association. The results obtained demonstrate the possibility of creating a siloxane network through managing the hydrolysis and subsequent condensation processes when developing technologies for flexible, transparent, and shape-stable gels.

Authors' contributions

A.M. Bondareva—conducting the experiments, discussion of the results.

I.I. Pashkin—discussion of the results.

A.V. Krylov—setting the task, discussing the results.

The authors declare no conflict of interest.

REFERENCES

1. Donato K.Z., Matějka L., Mauler R.S., Donato R.K. Recent Applications of Ionic Liquids in the Sol–Gel Process for Polymer–Silica Nanocomposites with Ionic Interfaces. *Colloids Interfaces*. 2018;1(1):5. http://doi.org/10.3390/colloids1010005
2. Sanchez C., Belleville P., Popall M., Nicole L. Applications of advanced hybrid organic-inorganic nanomaterials: From laboratory to market. *Chem. Soc. Rev.* 2011;40(2):696–753. https://doi.org/10.1039/c0cs00136h
3. Brinker C.J., Scherer G.W. *Sol–Gel Science: The Physics and Chemistry of Sol–Gel Processing.* Elsevier; 1990, 908 p.
4. Matějka L. Epoxy-silica/silsesquioxane Polymer Nanocomposites. In: Merhari L. (Ed.). *Hybrid Nanocomposites for Nanotechnology*. Boston, MA, USA: Springer; 2009. P. 1–84. http://doi.org/10.1007/978-0-387-30428-1_1
5. Pajonk G.M., Elaloui E., Chevalier B., Begag R. Optical transmission properties of silica aerogels prepared from polyethoxidisiloxanes. *J. Non-Crystalline Solids*. 1997;210(2-3): 224–231. http://doi.org/10.1016/S0022-3093(96)00600-X
6. Danks A.E., Hall S.R., Schnepp Z. The evolution of "sol–gel" chemistry as a technique for materials synthesis. *Mater. Horiz*. 2016;3(2):91–112. https://doi.org/10.1039/c5mh00260e
7. Pagliaro M., Ciriminna R., Palmisano G. Silica-based hybrid coatings. *J. Mater. Chem*. 2009;19(20):3116–3120. https://doi.org/10.1039/B819615J
8. Nassif N., Livage J. From diatoms to silica-based biohybrids. *Chem. Soc. Rev*. 2011;40(2):849–859. https://doi.org/10.1039/c0cs00122h
9. Vallet-Regi M., Colilla M., Gonzalez B. Medical applications of organic-inorganic hybrid materials within the field of silica-based bioceramics. *Chem. Soc. Rev.* 2011;40:596-607. https://doi.org/10.1039/c0cs00025f
10. Li J., Mooney D.J., Buffle J., DeRouchey J.E., Langer R. Designing. Hydrogels for Controlled Drug Delivery. *Nat. Rev. Mater*. 2016;1(12):16071. https://doi.org/10.1038/natrevmats.2016.71
11. Slaughter B.V., Khurshid S.S., Fisher O.Z., Khademhosseini A., Peppas N.A. Hydrogels in Regenerative Medicine. *Adv. Mater.* 2009;21(32-33):3307–3329. https://doi.org/10.1002/adma.200802106
12. Hayashi K., Okamoto F., Hoshi S., *et al*. Fast-Forming Hydrogel with Ultralow Polymeric Content as an Artificial Vitreous Body. *Nat. Biomed. Eng*. 2017;1(3):0044. https://doi.org/10.1038/s41551-017-0044
13. Peppas N.A., Hilt J.Z., Khademhosseini A., Langer R. Hydrogels in Biology and Medicine: From Molecular Principles to Bionanotechnology. *Adv. Mater*. 2006;18(11):1345–1360. https://doi.org/10.1002/adma.200501612
14. Letailleur A.A., Ribot E., Boissiere C., Teisseire J., Barthel E., Desmazieres B., Chemin N., Sanchez C. Sol–gel derived hybrid thin films: The chemistry behind processing. *Chem. Mater.* 2011;23:5082–5089. http://doi.org/10.1021/cm202755g
15. Sanchez C., Shea K.J., Kitagawa S. Recent progress in hybrid materials science. *Chem. Soc. Rev.* 2011;40(2):471–472. https://doi.org/10.1039/c1cs90001c
16. Avnir D., Levy D., Reisfeld R. The nature of the silica cage as reflected by spectral changes and enhanced photostability of trapped Rhodamine 6G. *J. Phys. Chem.* 1984;88(24): 5956–5959. https://doi.org/10.1021/j150668a042
17. Owens G.J., Singh R.K., Foroutan E, Alqaysi M., Han C.M., Mahapatra C., Kim H.W., Knowles J.C. Sol–gel based materials for biomedical applications. *Prog. Mater. Sci*. 2016;77:1–79. https://doi.org/10.1016/j.pmatsci.2015.12.001
18. Lu A.H., Schüth F. Nanocasting: A versatile strategy for creating nanostructured porous materials. *Adv. Mater*. 2006;18(14): 1793–1805. https://doi.org/10.1002/adma.200600148
19. Jiang P., Bertone J.F., Colvin V.L. A Lost-Wax Approach to Monodisperse Colloids and Their Crystals. *Science*. 2001; 291(5503):453–457. https://doi.org/10.1126/science.291.5503.453
20. Díaz-García M.E., Laíñ R.B. Molecular Imprinting in Sol–Gel Materials: Recent Developments and Applications. *Microchim. Acta*. 2005;149(1-2):19–36. https://doi.org/10.1007/s00604-004-0274-7
21. Chen L., Wang X., Lu W., Wu X., Li J. Molecular imprinting: Perspectives and applications. *Chem. Soc. Rev.* 2016;45(8):2137–2211. https://doi.org/10.1039/c6cs00061d
22. Guan Z.S., Lu C.H., Zhang Y., Xu Z.Z. Morphology-controlled Synthesis of SiO_2 Hierarchical Structures Using Pollen Grains as Templates. *Chinese J. Chem*. 2008;26(3):467–470. https://doi.org/10.1002/cjoc.200890088
23. Rahman I.A., Padavettan V. Synthesis of Silica nanoparticles by sol–gel: Size-dependent properties, surface modification, and applications in silica-polymer nanocomposites: A review. *J. Nanomater.* 2012:132424. https://doi.org/10.1155/2012/132424
24. Jindal A., Vasudevan S. The Conformation of Ethylene Glycol in the Liquid State: Intra- Versus Intermolecular Interactions. *J. Phys. Chem. B*. 2017;121(22):5595–5600. https://doi.org/10.1021/acs.jpcb.7b02853
25. Klingshirn M.A., Spear S.K., Subramanian R., Holbrey J.D., Huddleston J.G., Rogers R.D. Gelation of Ionic Liquids Using a Cross-Linked Poly(Ethylene Glycol) Gel Matrix. *Chem. Mater.* 2004;16(16):3091–3097. https://doi.org/10.1021/cm0351792
26. Andrade-Espinosa G., Escobar-Barrios V., Rangel-Mendez R. Synthesis and characterization of silica xerogels obtained via fast sol–gel process. *Colloid Polym. Sci.* 2010;288(18): 1697–1704. https://doi.org/10.1007/s00396-010-2311-x
27. Perullini M., Jobbagy M., Bilmes S.A., Torriani I.L., Candal R. Effect of synthesis conditions on the microstructure of TEOS derived silica hydrogels synthesized by the alcohol-free sol–gel route. *J. Sol–Gel Sci. Technol.* 2011;59(1):174–180. https://doi.org/10.1007/s10971-011-2478-8
28. Zhang H.N., Zhao Y., Akins D.L. Synthesis and new structure shaping mechanism of silica particles formed at high pH. *J. Solid State Chem.* 2012;194:277–281. https://doi.org/10.1016/j.jssc.2012.05.031
29. Zhao B.B., Tian C.H., Zhang Y., Tang T., Wang F.Y. Size control of monodisperse nonporous silica particles by seed particle growth. *Particuology*. 2011;9(3):314–317. https://doi.org/10.1016/j.partic.2010.07.028
30. Bogush G.H., Zukoski C.F Studies of the Kinetics of the Precipitation of Uniform Silica Particles through the Hydrolysis and Condensation of Silicon Alkoxides. *J. Colloids Interface Sci.* 1991;142(1):1–18. https://doi.org/10.1016/0021-9797(91)90029-8
31. Harris M.T., Byers C.H., Brunson R.R. The base-catalyzed hydrolysis and condensation reactions of dilute and concentrated TEOS solutions. *J. Non-Cryst. Solids*. 1990;121(1-3):397–403. https://doi.org/10.1016/0022-3093(90)90165-I
32. Lee K., Look J.L., Harris M.T., McCormick A.V. Assessing Extreme Models of the Stöber Synthesis Using Transients under a Range of Initial Composition. *J. Colloid Interface Sci.* 1997;194(l):78–88. https://doi.org/10.1006/jcis.1997.5089
33. Brinker C.J., Keefer K.D., Schaefer D.W., Assink R.A., Kay E.D., Ashley C.S. Sol–gel transition in simple silicates II. *J. Non-Cryst. Solids*. 1984;63(l-2):45–59. http://doi.org/10.1016/0022-3093(84)90385-5
34. Prabakar P., Assink R.A., Irwin A.D. Spinnability of Silica Sols: the Role of Alkoxy Group Exchange. *Mater. Res. Soc. Symp. Proc*. 1994;346:433–437. https://doi.org/10.1557/PROC-346-433

35. Schmidt H., Rinn G., Nass R., Sporn D. Film Formation by Inorganic-Organic Sol–Gel Synthesis. In: *Better Ceramics through Chemistry III*. 1988;121:743–752. *MRS Online Proceedings Library*. https://doi.org/10.1557/PROC-121-743
36. Green D.L., Jayasundara S., Lam Y.-F., Harris M.T. Chemical reaction kinetics leading to the first Stober silica nanoparticles – NMR and SAXS investigation. *J. Non-Cryst. Solids*. 2003;315(1-2): 166–179. http://doi.org/10.1016/S0022-3093(02)01577-6
37. Malay O., Yilgor I., Yusuf Z., Menceloglu Yu.Z. Effects of solvent on TEOS hydrolysis kinetics and silica particle size under basic conditions. *J. Sol-Gel. SciTechnol*. 2013;67(2): 351–361. https://doi.org/10.1007/s10971-013-3088-4
38. Bari A.H., Jundale R.B., Kulkarnia A.A. Understanding the role of solvent properties on reaction kinetics for synthesis of silica nanoparticles. *Chem. Eng. J.* 2020;398(9):125427. http://doi.org/10.1016/j.cej.2020.125427
39. Bernards T.N.M., Janssen M.J.C.H., van Bommel M.J. Influence of butanol on the hydrolysis-condensation behaviour of TEOS. *J. Non-Cryst. Solids*.1994;168(3):201–212. http://doi.org/10.1016/0022-3093(94)90331-X
40. Lim J.H., Ha S.W., Lee J.K. Precise Size-control of Silica Nanoparticles via Alkoxy Exchange Equilibrium of Tetraethyl Orthosilicate (TEOS) in the Mixed Alcohol Solution. *Bull. Korean Chem. Soc*. 2012;33(3):1067–1070. https://doi.org/10.5012/bkcs.2012.33.3.1067
41. Dyment O.N., Kazanskii K.S., Miroshnikov A.M. *Glikoli i drugie proizvodnye okisei ehtilena i propilena* (*Glycols and Other Derivatives of Ethylene and Propylene Oxides*). Moscow: Khimiya; 1976, 373 p. (in Russ.).

About the Authors

Alevtina M. Bondareva, Postgraduate Student, Ya.K. Syrkin Department of Physical Chemistry, M.V. Lomonosov Institute of Fine Chemical Technologies, MIREA – Russian Technological University (78, Vernadskogo pr., Moscow, 119454, Russia). E-mail: bondaalevtina@yandex.ru. https://orcid.org/0009-0006-0243-9289

Igor I. Pashkin, Cand. Sci. (Chem.), Chief Specialist, S.S. Medvedev Department of Chemistry and Technology of Macromolecular Compounds, M.V. Lomonosov Institute of Fine Chemical Technologies, MIREA – Russian Technological University (78, Vernadskogo pr., Moscow, 119454, Russia). E-mail: pashkin@mirea.ru. RSCI SPIN-code 7626-7693, https://orcid.org/0000-0002-5315-6370

Alexander V. Krylov, Cand. Sci. (Chem.), Associate Professor, Ya.K. Syrkin Department of Physical Chemistry, M.V. Lomonosov Institute of Fine Chemical Technologies, MIREA – Russian Technological University (78, Vernadskogo pr., Moscow, 119454, Russia). E-mail: allylnmr@yandex.ru. Scopus Author ID 57484351900, RSCI SPIN-code 5633-1360, https://orcid.org/0000-0002-2389-9026

Об авторах

Бондарева Алевтина Михайловна, аспирант, кафедра физической химии им. Я.К. Сыркина, Институт тонких химических технологий им. М.В. Ломоносова, ФГБОУ ВО «МИРЭА – Российский технологический университет» (119454, Россия, Москва, пр-т Вернадского, д. 78). E-mail: bondaalevtina@yandex.ru. https://orcid.org/0009-0006-0243-9289

Пашкин Игорь Иванович, к.х.н., главный специалист, кафедра химии и технологии высокомолекулярных соединений им. С.С. Медведева, Институт тонких химических технологий им. М.В. Ломоносова, ФГБОУ ВО «МИРЭА – Российский технологический университет» (119454, Россия, Москва, пр-т Вернадского, д. 78). E-mail: pashkin@mirea.ru. SPIN-код РИНЦ 7626-7693, https://orcid.org/0000-0002-5315-6370

Крылов Александр Владимирович, к.х.н., доцент, кафедра физической химии им. Я.К. Сыркина, Институт тонких химических технологий им. М.В. Ломоносова. ФГБОУ ВО «МИРЭА – Российский технологический университет» (119454, Россия, Москва, пр-т Вернадского, д. 78). E-mail: allylnmr@yandex.ru. Scopus Author ID 57484351900, SPIN-код РИНЦ 5633-1360, https://orcid.org/0000-0002-2389-9026

Translated from Russian into English by N. Isaeva
Edited for English language and spelling by Dr. David Mossop